buildings

Article

Using Optimization Algorithms-Based ANN to Determine the Temperatures in Timber Exposed to Fire for a Long Duration

Mehdi Nikoo [1], Ghazanfarah Hafeez [1] and Paulo Cachim [2,*]

[1] Department of Building, Civil and Environmental Engineering, Concordia University, Montréal, QC H3G 1M8, Canada
[2] RISCO, Department of Civil Engineering, University of Aveiro, 3810-193 Aveiro, Portugal
* Correspondence: pcachim@ua.pt; Tel.: +351-234370097

Abstract: The article investigates the temperature prediction in rectangular timber cross-sections exposed to fire. Timber density, exposure time, and the point coordinates within the cross-section are treated as inputs to determine the temperatures. A total of 54,776 samples of wood cross-sections with a variety of characteristics were considered in this study. Of the sample data, 70% was dedicated to training the networks, while the remaining 30% was used for testing the networks. Feed-forward networks with various topologies were employed to examine the temperatures of timber exposed to fire for more than 1500 s. The weight of the artificial neural network was optimized using bat and genetic algorithms. The results conclude that both algorithms are efficient and accurate tools for determining the temperatures, with the bat algorithm being marginally superior in accuracy than the genetic algorithm.

Keywords: temperatures; timber; fire; artificial neural network; optimization algorithms

check for updates

Citation: Nikoo, M.; Hafeez, G.; Cachim, P. Using Optimization Algorithms-Based ANN to Determine the Temperatures in Timber Exposed to Fire for a Long Duration. *Buildings* **2022**, *12*, 2265. https://doi.org/10.3390/buildings12122265

Academic Editor: Flavio Stochino

Received: 28 November 2022
Accepted: 16 December 2022
Published: 19 December 2022

1. Introduction

The behavior of timber under fire exposure is a critical factor in structural design [1]. Eurocode 5 (2004) [2] offers two simplified and one advanced calculation method for various fire situations. However, these methods do not account for some critical parameters, including timber density and the resultant stress in the cross-section [1–3].

Cachim predicted timber temperatures under fire loading using ANNs. He trained and tested the ANNs using numerical values obtained from the Eurocode 5 (2004) advanced design method to calculate timber temperatures subjected to fire loading. The author employed feed-forward modelling for testing and training the models. The resulting ANN-based model demonstrated accurate temperature prediction of fire-exposed timber members [4]. Lineham et al. conducted a unique series of fire experiments on CLT beams. They compared load-bearing capacities and recorded deflection time histories during heating to predict responses using experimentally determined char depths. The results demonstrated that the existing value for the zero-strength layer does not capture the requisite physics for robust structural response prediction under non-standard heating [5].

Buchanan focused on the structural performance of both light and heavy timber buildings exposed to fires, considering pre- and post-flashover fires [6]. Fragiacomo investigated a numerical model to predict the fire resistance of timber beams made from laminated veneer lumber under a tensile load. The effect of fire, considered as a reduction in modulus of elasticity and strength, was already assessed in a time-dependent thermal analysis. The prediction of fire resistance was found to be reasonable, with the difference being only 5% between the numerical and experimental results [7]. Schmid and Frangi investigated the fire dynamics and heat stored in the char layer as a critical factor for buildings exposed to fire. They also focused on the effect of an additional fire load from other structural linear components like beams and columns. Their validation is followed by existing experiments, and the developed model could predict the burnout and the charring depth within acceptable limits [8].

Naser developed temperature-dependent material models for tracing the thermostructural reaction of timber elements/components using artificial intelligence (AI). The author identified the importance of employing AI to modernize fire resistance evaluation by demonstrating the high degree of perception in AI models [9]. Audebert et al. conducted a comprehensive experimental and computational study based on fire testing of timber connections subjected to various mechanical loads. They generated numerical models to simulate the thermomechanical behavior of the tested timber connections [10]. Bai et al. investigated the load-bearing capacity of cross-laminated timber walls subjected to fire. Additionally, they demonstrated that numerical models could accurately reproduce the failure process and mechanical behavior of the studied CLT specimens. They conducted a parametric prediction using numerical methods to determine the effect of the number of layers and the combustion time on the residual load-carrying capacity following fire [11].

Szász et al., using a timber-steel-timber connection, investigated the behavior of double-sheared dowelled connections under temporal variations in fire performance. The authors examined the performance of the applied fire curve, the timber cross-section's width, and the fasteners' diameter [12].

Numerous articles have been published using finite element in the field of loading due to fire and its analysis, including those on thermo-mechanically compressed spruce timber [13], heat transfer through timber elements [14], timber columns [15,16], and a timber wall [17–19]. It has been observed that all of the aforementioned studies employed numerical models and artificial neural networks for finding solutions to complex situations.

In this article, the authors investigated the long-duration time and the relevant scientific analyses, which have not been previously addressed, employing a variety of algorithms implemented in ANN. Further, the authors realize that the development of artificially intelligent models leads to fewer samples being evaluated in the laboratories, ultimately reducing the project cost. The current study considers a metaheuristic algorithm to optimize the weights of the artificial neural network that yield the best solutions. The temperature of fire-exposed timber is determined using a feed-forward artificial neural networks bat algorithm, and a genetic algorithm is used to optimize the weight in artificial neural networks with different topologies. The best-performing model is then selected and evaluated for its accuracy.

2. Background

2.1. Temperatures in Timber under Fire Exposure

Fire is the most severe and fast process by which timber degrades and, thus, needs to be considered in the design of timber constructions. To perform a structural analysis of a timber structure, the distribution of temperatures in the cross sections after a certain period (typically 30 or 60 min) is mandatory as an alternative to simplified design rules. The advanced design method implies the use of advanced finite element software. In addition, experimental data with temperature evolution within timber elements exposed to fire conditions are not readily available. The use of ANN to model temperature distribution in timber cross sections based on numerical results comes as an interesting method to consider, in this context. The scarcity of data on temperatures in timber cross sections exposed to fire can be facilitated by employing numerical simulations based on advanced calculation methods [3]. These advanced calculation methods are based on the fundamentals of heat transfer and consider variations in thermal properties and the density of wood with temperature. Timber cross sections, under fire exposure, encounter critical effects, including water transfer within the wood and degradation of the material; these effects are accounted for as the modified equivalent properties of timber.

2.2. Artificial Neural Networks

An artificial neural network (ANN) comprises artificial neurons that collectively solve a unique problem. An ANN is a data processor that learns from experience. The model is based on the anatomy of the human brain and hence functions sufficiently when confronted with complications for which standard computational approaches fail, providing a convenient solution [20,21]. An ANN is typically composed of three distinct layers: the input layer, the hidden layer, and the output layer. Many researchers recommend using a single hidden layer in the ANN since a single layer with several nodes can predict input and output relationships with high accuracy [22]. We have used the same recommendation in the present study (two hidden layers). Each layer contains weighted connections that connect each neuron to several other nodes. The weights are trained in the ANN to be as close to the output values as possible [21].

The feed-forward network is a type of ANN in which the connections between its components do not form a cycle. This network is distinguished from recurrent neural networks because data only flows in one direction. Data begins with input nodes and progresses via hidden layers to the output nodes [20]. ANN data is typically divided into training and testing subgroups [23].

2.3. Bat Algorithm

Bats can avoid obstacles and identify prey by exploiting their remarkable echolocation capabilities. They create a three-dimensional representation of their environment by utilizing the temporal delay between pulse production and its echo [24]. Yang constructed the bat algorithm (BA) in response to this behavior of bats, assuming [25]:

- ➢ Bats employ echolocation and can discriminate between prey and the environment.
- ➢ At each given position xi, they fly randomly with velocity vi and modify their pulse emission rate in response to the prey's location.
- ➢ The emitted pulse has a loudness that varies from A0 to a minimum value of Amin.

BA begins by initializing a random population of bats and then updating their frequencies under Equation (1) [26]:

$$f_i = f_{min} + (f_{max} - f_{min})\beta \tag{1}$$

where f_i is the ith bat frequency, f_{min} is the min frequency, f_{max} is the max frequency, and β is a random value between 0 and 1. Equations (2) and (3) are used to modify the position and velocity of the bats [26]:

$$V_i^{t+1} = V_i^t + \left(x_i^t - \mathrm{x}^*\right) f_i \tag{2}$$

$$x_i^{t+1} = x_i^t + V_i^{t+1} \tag{3}$$

where V_i^t is the i-th bat velocity at recurrence t, x_i^t is the i-th bat position at recurrence t, and x^* is the global best position. The algorithm subsequently relocates some bats to an area around the top global location using Equation (4) [26]:

$$x_{new} = x_{old} + \varepsilon A^t \tag{4}$$

where A signifies loudness and ε is a random value between 0 and 1. The cost value of the new position of each bat must be smaller than the previous iteration's cost value. Following that, the algorithm modifies the pulse rate and volume using Equations (5) and (6) [26]:

$$A_i^{t+1} = \alpha A_i^t \tag{5}$$

$$r_i^{t+1} = r_i^0 (1 - \exp(-\gamma t)) \tag{6}$$

where α is a fixed value between zero and one, r_i^0 is the initial pulse rate, and γ is a fixed value.

This approach can be used to train an artificial neural network. In these applications, the weights and biases of the network are treated as the position vector of a bat, and so each bat reflects a vector of weights from an ANN. The cost function represents the network's prediction error. The bat algorithm's ultimate solution produces a trained network, as seen in Figure 1 [26,27].

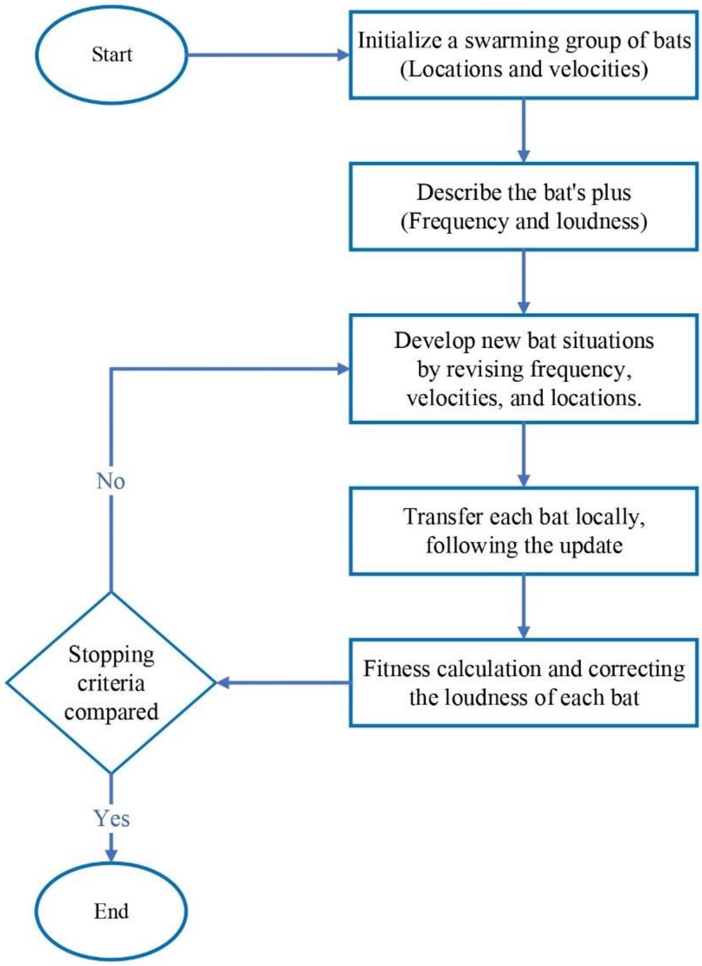

Figure 1. Flowcharts of the bat algorithm process.

2.4. Genetic Algorithm (GA)

In GA, the chromosomes with a high level of competence have a greater chance of reproducing in the selected population throughout the reproduction process, accomplished by employing the selection process [28]. Later, the operator is applied to the preferred reproduction direction, and a random number is created for each chromosome during the transplantation procedure at a steady pace. If the generated random number is less than the transplant rate, this chromosome is chosen to interact with the next chromosome per the above parameters. This strategy employs uniform transplanting across various transplantations followed by implementation of the mutation operator [29], which attempts to increase the dispersion of design space. Natural genetics' three fundamental operators are reproduction, crossover, and mutation. The GA can be stated as seen in Figure 2 [29]. GA is concluded when certain conditions, such as the number of generations or the average standard deviation of individual performance, are met [29].

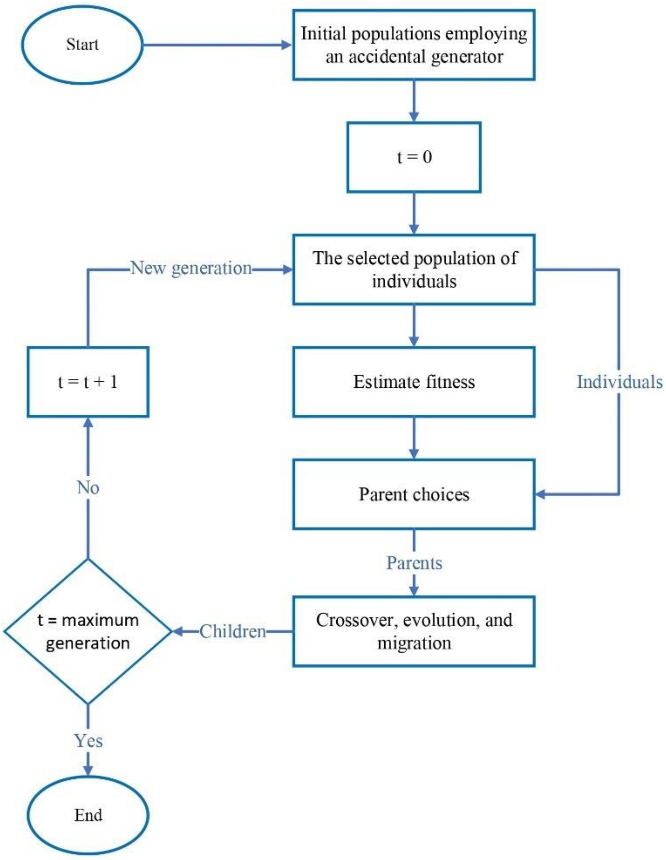

Figure 2. Flowcharts of genetic algorithm process.

2.5. Performance Measures

The network results can be verified using several error metrics comparing the disparities between the network's predictions and the data outputs. The average absolute error (AAE) and the mean absolute error (MAE) are two often used error measurements with Equations (7) and (8) [1,30,31]:

$$AAE = \frac{\sum_{i=1}^{n} \left| \frac{(O_i - P_i)}{O_i} \right|}{n} \tag{7}$$

$$MAE = \frac{1}{n} \sum_{i=1}^{n} |P_i - O_i| \tag{8}$$

where P_i and O_i signify predicted and observational data, while n embodies the number of cases [30].

3. Methods and Materials

3.1. Dataset

A total of 54,776 samples with varying characteristics were used in this study, and the statistical parameters are listed in Table 1 [1]. The input parameters are the size of the cross-section (b_x, b_y), the coordinates of the point within the cross-section (d_x, d_y), the time of fire exposure (t), and the timber density (ρ). The size of the cross-section is important to characterize the geometry of the problem, and the timber density is important because the fire behavior of timber changes with density, so different timbers were studied. The coordinates of the point within the cross-section and time allow for the characterization of the evolution of temperatures within the cross-section. The dataset was obtained by performing parametric numeric calculations, using software SAFIR [32,33], for different cross-section sizes and timber densities for a total time of 60 min of standard fire exposure, with temperatures recorded every five minutes. SAFIR is a special purpose finite element code developed at the University of Liege for studying structures subjected to fire. Different materials, such as steel, concrete, timber, aluminium, gypsum, or thermally insulating products, can be used separately or in combination in the model. The software calculates the temperatures in the cross sections, updating the mechanical properties accordingly. It can be used to just evaluate the temperatures in the cross sections or to model the overall structural behavior. Six characteristics, including the cross-section's size, timber density, exposure time, and the coordinates of the cross-section's point, are used as input variables to calculate the temperatures within a timber cross-section. Considering the significant effect heat has on wooden structures over time, this study investigates the damage caused by times exceeding 1500 s (25 min). All four faces of the cross sections were exposed to the fire; due to the symmetrical cross section, the analyses were performed on one-fourth of the timber cross section. The standard nominal fire curve was employed to evaluate the cross sections.

Table 1. Statistical characteristics of the input and output parameters [1].

Parameter	Abbreviation	Unit	Type	Max	Min	STD	Average	Mode
The timber density	ρ	$\frac{kg}{m^3}$	Input	800.0	350.0	169.7	550.7	800.0
The size of the cross section	b_x	mm	Input	300.0	120.0	71.5	199.4	120.0
	b_y	mm	Input	300.0	120.0	73.1	250.8	300.0
Time	t	s	Input	3600.0	1500.0	684.1	2540.0	2700.0
The coordinates of the point within the cross section	d_x	mm	Input	150.0	0.0	36.6	49.9	0.0
	d_y	mm	Input	150.0	0.0	42.9	62.7	60.0
Temperature	Temp	°C	Output	945.2	20.0	360.1	416.5	20.0

Clustering analysis is a classification method that groups the input parameters based on their narrow association, keeping similar data within a group. This grouping can vary depending on the input variables. As shown in Figure 3, three groups are created with the most influential parameters: the timber density (ρ) in the first group, time (t) in the second group, the size of the cross-section (b_x, b_y) and the coordinates of the point within the cross-section (d_x, d_y) in the third group.

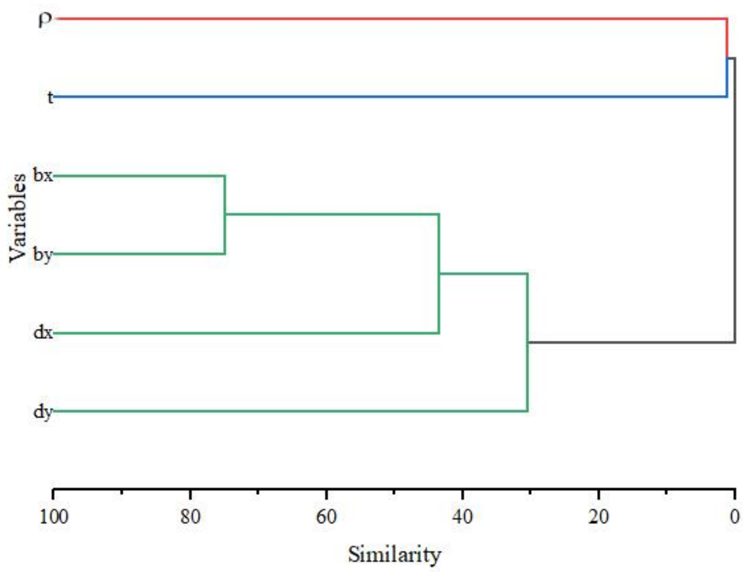

Figure 3. Clustering analysis for the input parameters.

A correlation matrix is a table that contains the correlation coefficients for various variables. The matrix represents correlations between all possible pairs of values in a table. It is an effective tool for summarizing large datasets and identifying the patterns within the data set. Correlation matrices are made up of rows and columns containing the variables. Correlation coefficients are stored in each cell of a table.

Furthermore, the correlation matrix is frequently combined with other forms of statistical analysis [34]. According to Figure 4, the variables d_x and d_y have a more significant effect on temperature than the ρ variable. However, all six variables affect temperature and will be considered in the models.

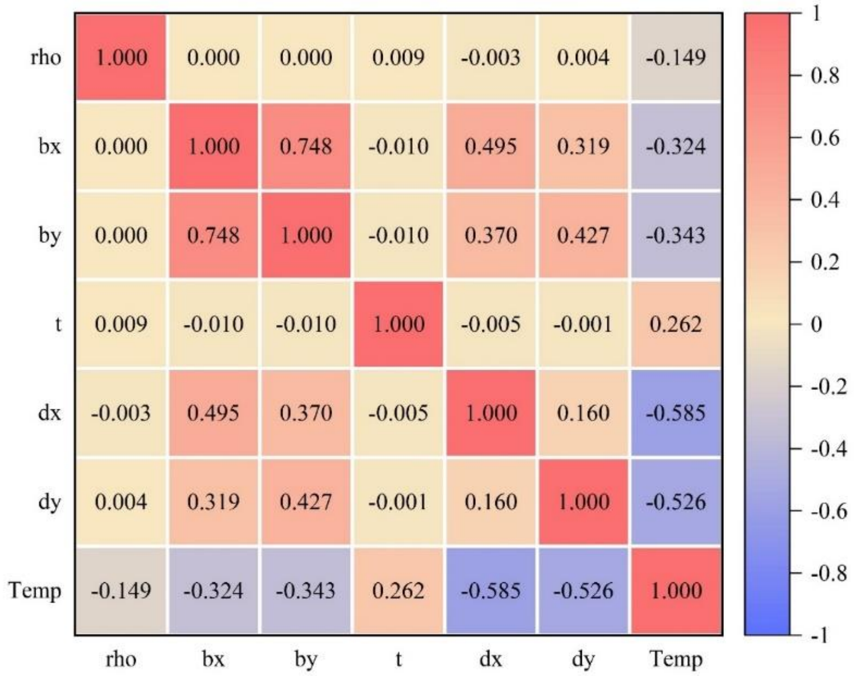

Figure 4. Correlation matrix for input and output variables.

3.2. Artificial Neural Network Combined with Genetic Algorithm

Feed-forward ANN models were used to calculate temperatures within a timber cross-section. In some cases, the neural network has very high accuracy and a low error rate in the training phase. However, it cannot show appropriate performance and fails to provide satisfactory results when placed in the test phase. The data were randomly separated into two sets to mitigate the impact of this event [35]. In this paper, out of 54,776 samples, 70% (38,343) of the samples were used for training, and the remaining 30% (16,433 samples) were used to test the performance of the networks. An experimental method was used to determine the number of hidden layers and neurons, given in Equation (9) [36].

$$N_H \leq \min(2N_I + 1) \tag{9}$$

where N_H is the number of hidden layer nodes, and N_I is the number of inputs. Considering the number of inputs equals 6 in Equation (9), the maximum number of nodes in the two hidden layers equals 13, and the different topologies are shown in Table 2. For all artificial neural networks, sigmoid, tangent sigmoid, purelin (linear), poslin (positive linear), and log sigmoid are considered transfer functions of the hidden and output layers. Also, to adjust the weights and biases in the neural network, the genetic algorithm was used to minimize the error. The characteristics of the genetic algorithm are presented in Table 3.

Table 2. Different topologies used in artificial neural networks.

No	Hidden Layer 1	Hidden Layer 2	Hidden Activations	Output Activation	No	Hidden Layer 1	Hidden Layer 2	Hidden Activation	Output Activation
1	7	6	TANSIG	PURELIN	11	5	4	TANSIG	PURELIN
2	7	5	TANSIG	TANSIG	12	5	3	TANSIG	TANSIG
3	7	4	POSLIN	PURELIN	13	4	6	POSLIN	PURELIN
4	7	3	LOGSIG	PURELIN	14	4	5	LOGSIG	PURELIN
5	6	6	PURELIN	PURELIN	15	4	4	PURELIN	PURELIN
6	6	5	TANSIG	PURELIN	16	4	3	TANSIG	PURELIN
7	6	4	TANSIG	TANSIG	17	3	6	TANSIG	TANSIG
8	6	3	POSLIN	PURELIN	18	3	5	POSLIN	PURELIN
9	5	6	LOGSIG	PURELIN	19	3	4	LOGSIG	PURELIN
10	5	5	PURELIN	PURELIN	20	3	3	PURELIN	PURELIN

Table 3. Parameters of the genetic algorithm [23].

Parameter	Value	Parameter	Value
Crossover (%)	50	Max generations	150
Crossover method	single-point	Recombination (%)	15
Lower bound	−1	Selection Mode	1
Upper bound	+1	Population Size	150

To determine the temperatures within a timber cross-section, among the 20 models used, the top three models were selected based on the MAE, AAE, R^2, and straight-line slope values, shown in Table 4.

Table 4. Statistics of the top three ANNs combined with GA for temperatures.

Model	Train				Test			
	MAE	AAE	R^2	y = ax + b	MAE	AAE	R^2	y = ax + b
GA-ANN 2L(7-6)	8.89	0.057	0.9985	y = 0.9989x + 0.4065	9.13	0.058	0.9985	y = 0.9984x + 0.6274
GA-ANN 2L(7-3)	8.20	0.048	0.9987	y = 0.9995x + 0.0775	8.17	0.051	0.9989	y = 0.9968x + 1.5171
GA-ANN 2L(6-5)	7.58	0.078	0.9990	y = 0.9988x + 0.5182	7.05	0.065	0.9991	y = 0.9994x + 0.1171

According to Table 4, the GA-ANN 2L network (6-5) has the lowest MAE and AAE values of 7.58 and 0.078 in the training stage, respectively, and 7.05 and 0.065 in the test stage, respectively. It also shows the highest R^2 value in each training and testing stage, equal to 0.9990 and 0.9991, respectively, indicating that the model performs better than the other nineteen. To illustrate the performance of GA-ANN 2L(6-5), Figures 5 and 6 demonstrate the computed values of the empirical model versus their observed values for training and testing, respectively. The values calculated by the model near the $y = x$ line indicate the model's accuracy.

3.3. Artificial Neural Network Combined with Bat Algorithm

The twenty architectures listed in Table 2 were trained using the bat algorithm (BA) parameter as provided in Table 5 to determine the best ANN architecture.

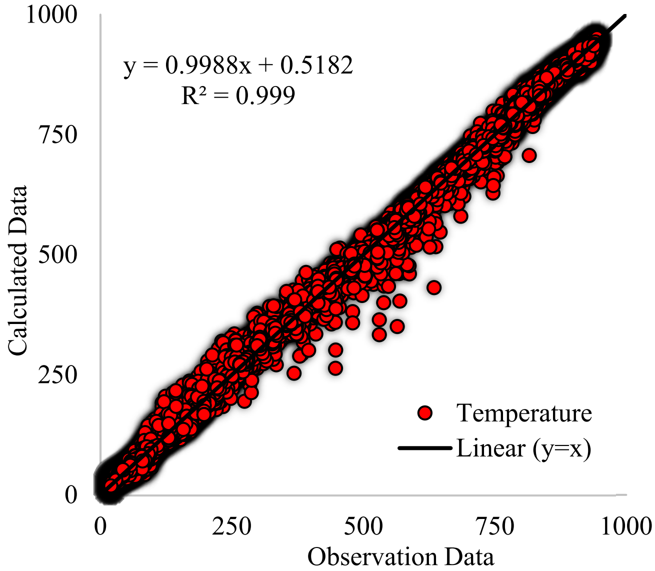

Figure 5. Comparison of the observed and calculated temperatures within a timber cross-section in the training phase using GA-ANN 2L(6-5).

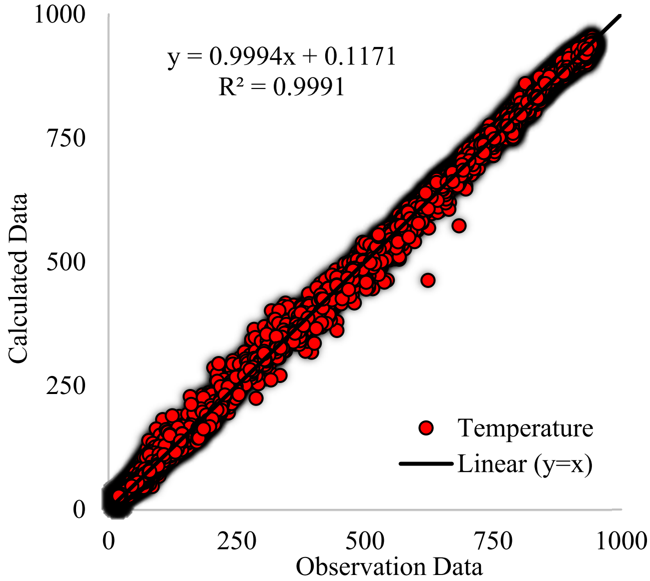

Figure 6. Comparison of the observed and calculated temperatures within a timber cross-section in the testing phase using GA-ANN 2L(6-5).

Table 5. Bat algorithm parameters [23].

Hyperparameter	Value	Hyperparameter	Value
Population Total	100	Max Generations	200
Loudness	0.9	Pulse Rate	0.5
Min Freq.	0	Max Freq.	2
Alpha	0.99	Gamma	0.01

The models were evaluated based on the MAE, AAE, and R^2 values. The top three best-performing models are shown in Table 6 with their respective statistical indices. As seen in Table 6, BA-ANN 2L(6-4) is the best-performing model among others. The calculated values of residual temperature vs. their target values are displayed in Figures 7 and 8 to illustrate the model's performance (8).

Table 6. Statistics of the top three ANNs combined with the bat algorithm for temperatures.

Model	Train				Test			
	MAE	**AAE**	$\mathbf{R^2}$	**y = ax + b**	**MAE**	**AAE**	$\mathbf{R^2}$	**y = ax + b**
BA-ANN 2L(7-6)	7.29	0.064	0.9990	y = 0.999x + 0.3987	7.40	0.062	0.9990	y = 0.9989x + 0.347
BA-ANN 2L(7-5)	6.71	0.040	0.9991	y = 0.9982x + 0.8113	6.77	0.040	0.9991	y = 0.9979x + 0.9512
BA-ANN 2L(6-4)	6.18	0.034	0.9992	y = 0.9992x + 0.2432	6.32	0.035	0.9992	y = 0.999x + 0.2412

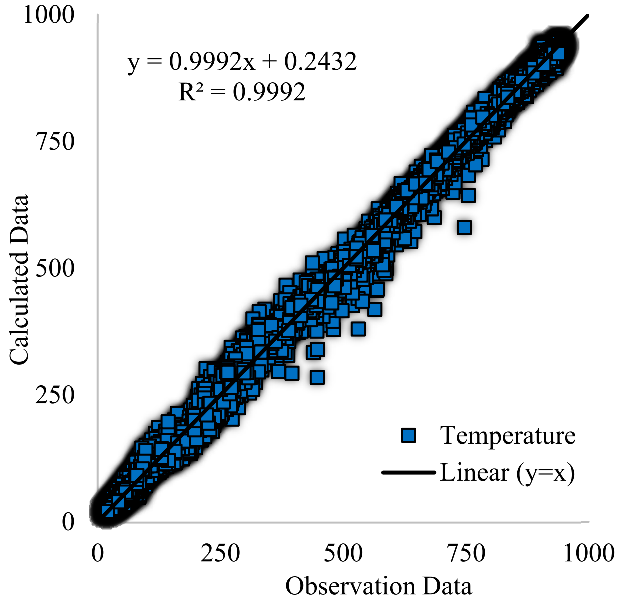

Figure 7. Comparison of the observed and calculated temperatures within a timber cross-section in the training phase using BA-ANN 2L(6-4).

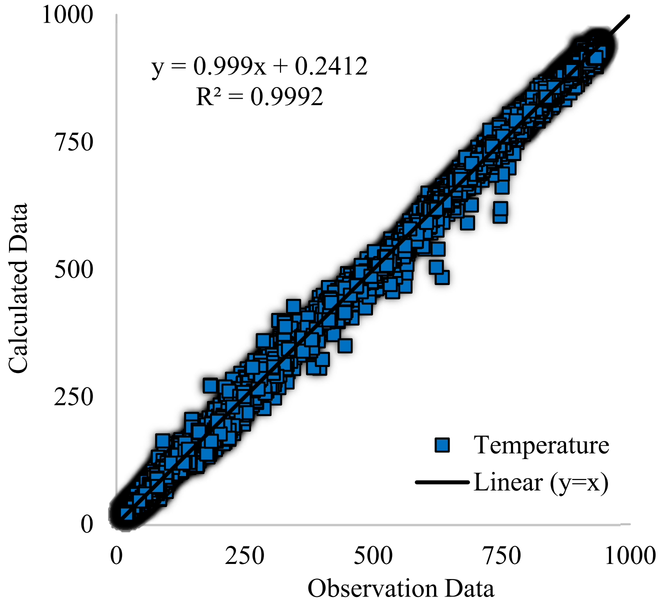

Figure 8. Comparison of the observed and calculated temperatures within a timber cross-section in the testing phase using BA-ANN 2L(6-4).

According to Table 6, BA-ANN 2L(6-5) has the lowest MAE and AAE values of 6.18 and 0.034 in the training stage, respectively, and 6.32 and 0.035 in the test stage, respectively. It also has the highest R^2 value in each training and testing stage, equal to 0.9992, which shows that the model is more accurate than the other 20 models of the same type.

3.4. Comparing All the Models and Choosing the Best Model

We evaluated the models on an equal basis for their performance. The evaluated models include BA-ANN and GA-ANN; the indicators used are AAE, MAE, R^2, and the straight-line slope, shown in Table 7. According to Figures 9 and 10, the BA-ANN 2L(6-4) model has the lowest MAE and AAE values, indicating higher accuracy, followed by the GA-ANN 2L(6-5) model.

Table 7. Statistical indices of different models in all datasets.

Model	All Dataset			
	MAE	**AAE**	**R^2**	**y = ax + b**
GA-ANN 2L(7-6)	8.96	0.058	0.9985	y = 0.9984x + 0.6274
GA-ANN 2L(7-3)	8.19	0.049	0.9988	y = 0.9987x + 0.5045
GA-ANN 2L(6-5)	7.42	0.074	0.9990	y = 0.999x + 0.3993
BA-ANN 2L(7-6)	7.32	0.064	0.9990	y = 0.999x + 0.3835
BA-ANN 2L(7-5)	6.73	0.040	0.9991	y = 0.9981x + 0.8528
BA-ANN 2L(6-4)	6.22	0.035	0.9992	y = 0.9992x + 0.2427

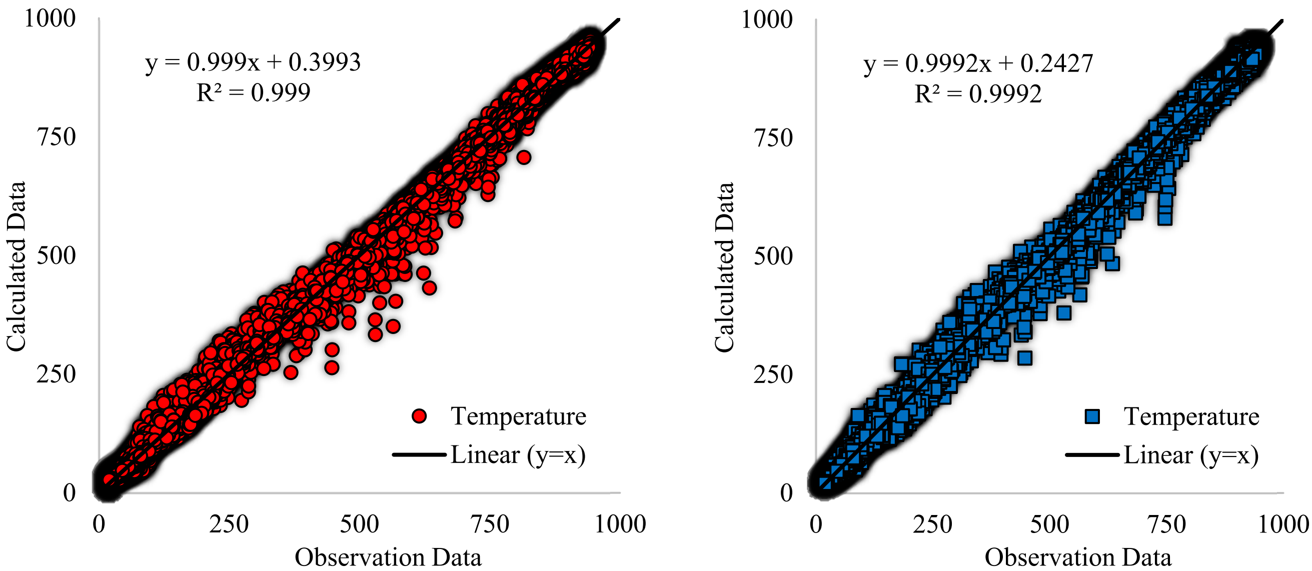

(**a**) (**b**)

Figure 9. Comparison of the observed and calculated temperatures within a timber cross-section in all datasets. (**a**) Genetic algorithm. (**b**) Bat algorithm.

The comparison of six models (three developed employing BA and three from GA) revealed that the BA-ANN2L(6-4) model was the best-performing model, followed by the GA-ANN 2L model (6-5). The artificial neural network optimized using the bat algorithm has much more flexibility and accuracy than the other models. The topology of the network is shown in Figure 11.

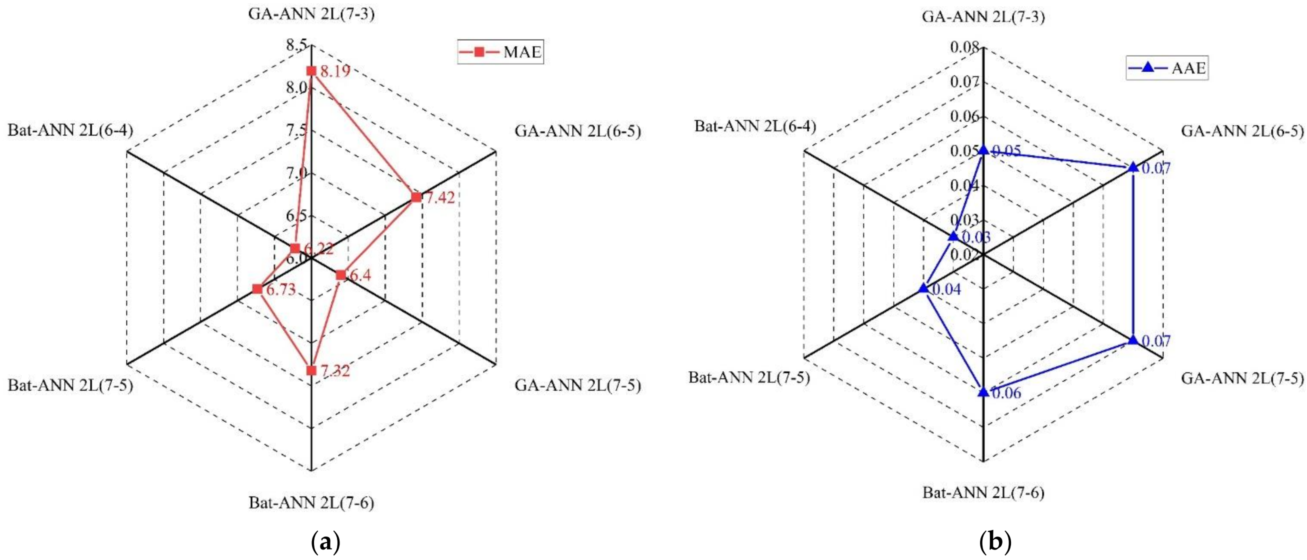

Figure 10. Statistical indices for the different models. (**a**). AAE (**b**). MAE.

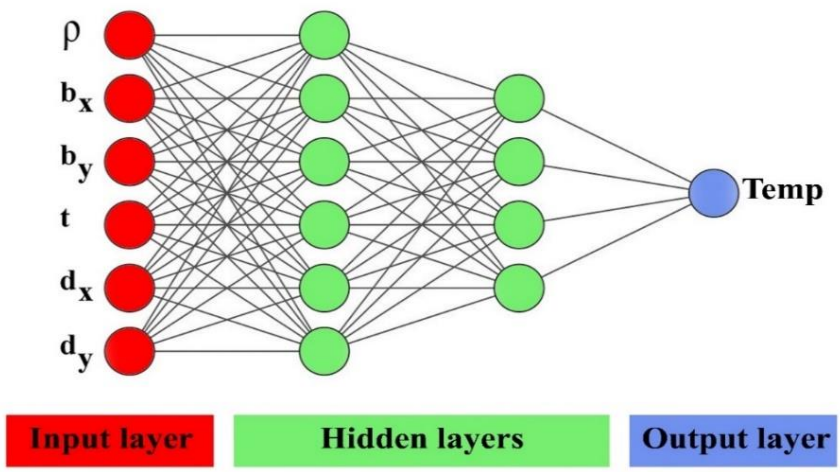

Figure 11. Best topology in a bat algorithm-based ANN.

4. Conclusions

This paper presents an ANN model optimized with bat and genetic algorithms for predicting the temperature. The bat algorithm was used to train 20 ANN models, whose input parameters were selected from the published dataset. The model's accuracy was evaluated by comparing the results with genetic algorithm models. Among the 20 models, the BA-ANN 2L(6-4) trained model is the most accurate model for predicting temperatures in rectangular timber cross-sections compared to other artificial neural networks with similar topologies. In the training data, MAE and AAE for temperatures were 6.18 and 0.034, respectively, while they returned 6.32 and 0.035 in the test data. The correlation coefficient R^2 for training and test data was 0.9992.

A genetic algorithm was used to optimize the ANN for determining the temperature of rectangular timber cross sections. The GA-ANN 2L model (6-5) had the most accurate topology compared to similar models. In the training data, the MAE and AAE values for temperatures were 7.58 and 0.078, respectively, while the test data returned 7.05 and 0.065, respectively. The correlation coefficients R^2 for training and test data were 0.9990 and 0.9991, respectively.

Both models optimized by the bat algorithm (BA-ANN 2L(6-4)) and genetic algorithm (GA-ANN 2L(6-5)) showed good performance for predicting the exposed timber. However, the model optimized by the bat algorithm demonstrated higher accuracy and lower error rates.

Author Contributions: M.N.: conceptualization, methodology, investigation, formal analysis, and writing—original draft preparation. G.H.: supervision, methodology, visualization, validation, writing, review, and editing. P.C.: experimental data, methodology, review, and editing. All authors have read and agreed to the published version of the manuscript.

Funding: This research was not supported by any specific grant from the public, commercial, or not-for-profit funding bodies.

Institutional Review Board Statement: Not applicable.

Informed Consent Statement: Not applicable.

Data Availability Statement: Not applicable.

Conflicts of Interest: The authors declare that they have no conflicting interest.

References

1. Cachim, P. ANN Prediction of Fire Temperature in Timber. *J. Struct. Fire Eng.* **2019**, *10*, 233–244. [CrossRef]
2. Cachim, P.B.; Franssen, J.-M. Numerical Modelling of Timber Connections under Fire Loading Using a Component Model. *Fire Saf. J.* **2009**, *44*, 840–853. [CrossRef]
3. *EN 1995-1-2:2004*; Eurocode 5: Design of Timber Structures–Part 1–2: General–Structural Fire Design. CEN: Brussels, Belgium, 2004.
4. Cachim, P.B. Using Artificial Neural Networks for Calculation of Temperatures in Timber under Fire Loading. *Constr. Build. Mater.* **2011**, *25*, 4175–4180. [CrossRef]
5. Lineham, S.A.; Thomson, D.; Bartlett, A.I.; Bisby, L.A.; Hadden, R.M. Structural Response of Fire-Exposed Cross-Laminated Timber Beams under Sustained Loads. *Fire Saf. J.* **2016**, *85*, 23–34. [CrossRef]
6. Buchanan, A.H. Fire Performance of Timber Construction. *Prog. Struct. Eng. Mater.* **2000**, *2*, 278–289. [CrossRef]
7. Fragiacomo, M.; Menis, A.; Moss, P.J.; Clemente, I.; Buchanan, A.H.; De Nicolo, B. Predicting the Fire Resistance of Timber Members Loaded in Tension. *Fire Mater.* **2013**, *37*, 114–129. [CrossRef]
8. Schmid, J.; Frangi, A. Structural Timber in Compartment Fires–The Timber Charring and Heat Storage Model. *Open Eng.* **2021**, *11*, 435–452. [CrossRef]
9. Naser, M.Z. Fire Resistance Evaluation through Artificial Intelligence-A Case for Timber Structures. *Fire Saf. J.* **2019**, *105*, 1–18. [CrossRef]
10. Audebert, M.; Dhima, D.; Bouchaïr, A. Proposal for a New Formula to Predict the Fire Resistance of Timber Connections. *Eng. Struct.* **2020**, *204*, 110041. [CrossRef]
11. Bai, Y.; Zhang, J.; Shen, H. Experimental and Numerical Analysis of Residual Load-Carrying Capacity of Cross-Laminated Timber Walls after Fire. *Structures* **2021**, *30*, 50–61. [CrossRef]
12. Szász, A.; Hlavička, V.; Lublóy, É.; Biró, A. Numerical Modelling of the Fire Resistance of Double Sheared Steel-to-Timber Connections. *J. Build. Eng.* **2021**, *37*, 102150. [CrossRef]
13. Tran, T.T.; Thi, V.-D.; Oudjene, M.; Khelifa, M.; Girods, P.; Debal, M.; Rogaume, Y.; Jannot, Y. Fire Structural Performance of Thermo-Mechanically Compressed Spruce Timber by Means Experiments and a Three-Step Multi-Reactions Pyrolysis 3D-Finite Element Modelling. *Constr. Build. Mater.* **2022**, *320*, 126100. [CrossRef]
14. Thi, V.D.; Khelifa, M.; Oudjene, M.; El Ganaoui, M.; Rogaume, Y. Finite Element Analysis of Heat Transfer through Timber Elements Exposed to Fire. *Eng. Struct.* **2017**, *143*, 11–21. [CrossRef]
15. Gernay, T. Fire Resistance and Burnout Resistance of Timber Columns. *Fire Saf. J.* **2021**, *122*, 103350. [CrossRef]
16. Palma, P.; Frangi, A. Modelling the Fire Resistance of Steel-to-Timber Dowelled Connections Loaded Perpendicularly to the Grain. *Fire Saf. J.* **2019**, *107*, 54–74. [CrossRef]
17. Bedon, C.; Fragiacomo, M. Experimental and Numerical Analysis of In-Plane Compressed Unprotected Log-Haus Timber Walls in Fire Conditions. *Fire Saf. J.* **2019**, *107*, 89–103. [CrossRef]
18. Thi, V.D.; Khelifa, M.; Oudjene, M.; El Ganaoui, M.; Rogaume, Y. Numerical Simulation of Fire Integrity Resistance of Full-Scale Gypsum-Faced Cross-Laminated Timber Wall. *Int. J. Therm. Sci.* **2018**, *132*, 96–103. [CrossRef]
19. Young, S.A.; Clancy, P. Structural Modelling of Light-Timber Framed Walls in Fire. *Fire Saf. J.* **2001**, *36*, 241–268. [CrossRef]
20. Khademi, F.; Jamal, S.M.; Deshpande, N.; Londhe, S. Predicting Strength of Recycled Aggregate Concrete Using Artificial Neural Network, Adaptive Neuro-Fuzzy Inference System and Multiple Linear Regression. *Int. J. Sustain. Built Environ.* **2016**, *5*, 355–369. [CrossRef]
21. Nikoo, M.; Hafeez, G. Artificial Neural Network Combined with Grey Wolf Optimizer for Period Determination of Light-Frame Wood Buildings. In Proceedings of the 7th International Conference on Architecture, Materials and Construction, Lisbon, Portugal, 27–29 October 2021; Mendonça, P., Cortiços, N.D., Eds.; Springer International Publishing: Cham, The Netherlands, 2022; pp. 213–222.
22. Deshpande, N.; Londhe, S.; Kulkarni, S. Modeling Compressive Strength of Recycled Aggregate Concrete by Artificial Neural Network, Model Tree and Non-Linear Regression. *Int. J. Sustain. Built Environ.* **2014**, *3*, 187–198. [CrossRef]

23. Aalimahmoody, N.; Bedon, C.; Hasanzadeh-Inanlou, N.; Hasanzade-Inallu, A.; Nikoo, M. BAT Algorithm-Based ANN to Predict the Compressive Strength of Concrete—A Comparative Study. *Infrastructures* **2021**, *6*, 80. [CrossRef]
24. Jun, L.; Liheng, L.; Xianyi, W. A Double-Subpopulation Variant of the Bat Algorithm. *Appl. Math. Comput.* **2015**, *263*, 361–377. [CrossRef]
25. Yang, X.S. *Nature-Inspired Optimization Algorithms*; Academic Press: Cambridge, MA, USA, 2014; ISBN 9780124167438.
26. Dehghani, H.; Bogdanovic, D. Copper Price Estimation Using Bat Algorithm. *Resour. Policy* **2018**, *55*, 55–61. [CrossRef]
27. Islam, T.; Ruhin, M.E.I.; Raihan, M. An Analysis of Foraging and Echolocation Behavior of Swarm Intelligence Algorithms in Optimization: ACO, BCO and BA. *Int. J. Intell. Sci.* **2018**, *8*, 82211. [CrossRef]
28. Nikoo, M.; Zarfam, P.; Sayahpour, H. Determination of Compressive Strength of Concrete Using Self Organization Feature Map (SOFM). *Eng. Comput.* **2015**, *31*, 113–121. [CrossRef]
29. Sadowski, L.; Nikoo, M. Corrosion Current Density Prediction in Reinforced Concrete by Imperialist Competitive Algorithm. *Neural Comput. Appl.* **2014**, *25*, 1627–1638. [CrossRef]
30. Li, J.; Heap, A.D. *A Review of Spatial Interpolation Methods for Environmental Scientists*; Geoscience Australia: Canberra, Australia, 2008; ISBN 9781921498305.
31. Keshtegar, B.; Ozbakkaloglu, T.; Gholampour, A. Modeling the Behavior of FRP-Confined Concrete Using Dynamic Harmony Search Algorithm. *Eng. Comput.* **2017**, *33*, 415–430. [CrossRef]
32. Franssen, J.-M. SAFIR: A Thermal/Structural Program for Modeling Structures under Fire. *Eng. J.* **2005**, *42*, 143–150.
33. Cachim, P.B.; Franssen, J.-M. Comparison between the Charring Rate Model and the Conductive Model of Eurocode 5. *Fire Mater.* **2009**, *33*, 129–143. [CrossRef]
34. Tosee, S.V.; Faridmehr, I.; Bedon, C.; Sadowski, Ł.; Aalimahmoody, N.; Nikoo, M.; Nowobilski, T. Metaheuristic Prediction of the Compressive Strength of Environmentally Friendly Concrete Modified with Eggshell Powder Using the Hybrid ANN-SFL Optimization Algorithm. *Materials* **2021**, *14*, 6172. [CrossRef]
35. Géron, A. *Hands-On Machine Learning with Scikit-Learn and TensorFlow: Concepts, Tools, and Techniques to Build Intelligent Systems*; O′Reilly Media, Inc.: Sebastopol, CA, USA, 2017.
36. Bowden, G.J.; Dandy, G.C.; Maier, H.R. Input Determination for Neural Network Models in Water Resources Applications. Part 1—Background and Methodology. *J. Hydrol.* **2005**, *301*, 75–92. [CrossRef]